

INTERACTION OF LASER RADIATION WITH MATTER. LASER PLASMA

PACS numbers: 52.50.Jm; 52.38.–r; 42.87.–d
DOI: 10.1070/QE2014v044n11ABEH015540

Investigation of free charge carrier dynamics in single-crystalline CVD diamond by two-photon absorption

E.V. Ivakin, I.G. Kisialiou, V.G. Ralchenko, A.P. Bolshakov, E.E. Ashkinazi, G.V. Sharonov

Abstract. **By using the methods of transient gratings (TGs) and induced absorption, we have studied the kinetics of plasma of free charge carriers (FCCs) created by the action of a picosecond laser pulse in two high-purity diamond single crystals synthesised from the gas phase. The gratings with different spatial periods have been excited at the wavelengths of 266 or 213 nm (above and below the fundamental absorption edge in diamond) and probed with continuous-wave radiation in the visible region. At the moderate FCC concentrations ($\sim 7\times10^{17}$ cm^{-3}), the coefficient of ambipolar diffusion and the carrier recombination time of two crystals are 20.3 and 18.9 cm^2 s^{-1} and 30 and 190 ns, respectively. The increase in the carrier concentration up to 5×10^{19} cm^{-3} reduces the TG lifetime. We have determined the conditions under which the relaxation of the grating of carriers leads to the formation of a thermal grating, with the amplitude sufficient for its experimental observation.**

Keywords: *CVD diamond, transient gratings, ambipolar diffusion, charge carriers, carrier lifetime.*

1. Introduction

One of the ways to control the electrical parameters of the materials in semiconductor electronics is the use of all-optical (laser) methods with a high temporal and spatial resolution [1–3]. Their peculiarity lies in the possibility of studying the electronic response of a sample to electromagnetic radiation of a relevant spectral range by the change in the optical parameters of material, conditioned by the generation of free charge carriers (FCCs). A prominent place here belongs to the method of transient gratings (TGs), in which the power of the exciting beam is periodically modulated in the volume or on the surface of the sample, and the signal is formed as a result of diffraction of the probe beam on the arising amplitude-phase grating.

E.V. Ivakin, I.G. Kisialiou B.I. Stepanov Institute of Physics, National Academy of Sciences of Belarus, prosp. Nezavisimosti 68, 220072 Minsk, Belarus; e-mail: ivakin@ifanbel.bas-net.by, i.kisialiou@gmail.com;
V.G. Ralchenko, A.P. Bolshakov, E.E. Ashkinazi A.M. Prokhorov General Physics Institute, Russian Academy of Sciences, ul. Vavilova 38, 119991 Moscow, Russia; e-mail: ralchenko@nsc.gpi.ru, bolshak@ran.gpi.ru, ashkinazi@nsc.gpi.ru;
G.V. Sharonov A.N. Sevchenko Institute of Applied Physical Problems, Belorussian State University, ul. Kurchatova 7, 220108 Minsk, Belarus; e-mail: sharonov@hotmail.ru

Received 21 April 2014; revision received 2 July 2014
Kvantovaya Elektronika **44** (11) 1055–1060 (2014)
Translated by M.A. Monastyrskiy

The TG method has been successfully used to study a number of semiconductors, such as GaAs:Cr, CdTe, Si [4, 5]. From the kinetics of diffraction of the probe beam one can determine directly two fundamental plasma parameters: the coefficient of ambipolar diffusion D and the FCC recombination time τ. According to the Einstein relation, in the case of thermal equilibrium and low external field intensity, there exists a simple analytical relationship [6] $D = \mu k T_{\rm abs} q^{-1}$ between the diffusion coefficient and the carrier mobility μ, where k is the Boltzmann constant; $T_{\rm abs}$ is the absolute temperature; and q is the electron charge. At room temperature, $D \approx 0.025\mu$ [7]. Unlike the electric methods of semiconductor research, the FCC motion after their generation occurs in the TG method not under the electric field influence, but as a result of the formed concentration gradient directed along the vector of the induced grating. Most often, this vector is oriented along the sample surface.

In recent years, the TG method has been successfully applied to the investigation of diamonds [8, 9], which is stipulated by the increasing interest in the use of this material in electronics, as well as the rapid development of the synthesis technology of diamonds from the gas phase by the CVD method. In the course of optical studies on the FCC dynamics in diamond, it was found that the results of measurements of the mobility and carrier lifetime are markedly different from those obtained by the conventional photoelectric method. In particular, according to the results of [7], the coefficient of ambipolar diffusion and the FCC lifetime in single-crystal CVD diamond with the concentration of nitrogen defects less than 10^{17} cm^{-3}, measured by the TG method at the FCC concentrations $N \approx 2\times10^{18}$ cm^{-3}, constituted 12 cm^2 s^{-1} and 3.3 ns, respectively. The same parameters measured by the time-of-flight method in the same sample at small ($N \approx 10^{13}$ cm^{-3}) carrier concentrations turned out significantly higher: 57 cm^2 s^{-1} or more than 10 ns.

Various physical processes may affect the charge carrier lifetime registered by the TG method [7]. Some of them are associated with the relatively high density of the FCCs, which is realised in the TG method. The present work is dedicated to the study of this concentration factor as applied to single crystal CVD diamond with a low content of nitrogen impurity. The investigations have been carried out in case of two-photon FCC excitation at a wavelength of 266 nm, which belongs to the transparency area of diamond (the edge of fundamental absorption is 225 nm). The idea of such measurements was formulated by in [10] and tested for IIa-type synthetic diamond crystals grown in a high-pressure apparatus [11]. The advantages of two-photon excitation are that, firstly, the FCC generation occurs in the sample bulk rather than in the near-surface layer as in the case of single-photon interband excitation,

and secondly, the FCC volume concentration decreases, whilst maintaining the diffraction efficiency of the electronic TGs at the level sufficient for the measurements.

The kinetics of the FCCs plasma absorption induced by two-photon pumping was additionally investigated. Furthermore, the TG excitation at a wavelength 213 nm was realised, which significantly increases the initial concentration of the charge carriers.

2. Description of samples and the optical scheme of the setup

We have studied two samples of monocrystalline diamond in the form of plane-parallel plates synthesised by deposition from the gas phase. The sample, hereinafter referred to as E6 (Element Six, UK), of high purity (the nitrogen content of no more than 5 ppb), had the dimensions of 4×4×0.5 mm with the surface roughness $R_a < 5$ nm. The second sample (No. 64/21) measuring 6×5×0.5 mm was epitaxially grown at the GPI RAS on a monocrystalline diamond substrate in microwave discharge (2.45 GHz) in the ARDIS-100 plasmochemical reactor (Optosystems Ltd) in a mixture of 4% CH_4–96% H_2 [12]. The process was carried out under the following parameters: microwave power of 2600 W, pressure of 130 Torr, total gas flow rate of 500 sccm, substrate temperature of 900 °C, growth rate of 9 μm h^{-1}. The synthesised layer was separated from the substrate by laser cutting and polished on both sides to the roughness $R_a < 10$ nm.

Figure 1 shows the transmittance spectra of both samples, obtained by the Cary 500 spectrometer (Varian) in the UV and visible regions, and the absorption spectra obtained by the Nexus Fourier spectrometer (Therm Nicolet) in the IR region. These spectra are virtually identical. The abrupt drop in transmittance at the wavelength of 225 nm corresponds to the fundamental absorption edge. The absorption bands in the IR region between 1600 and 3800 cm^{-1} correspond to the two- and three-phonon absorption and are not associated with defects. In the range of 230–300 nm and 7–10 μm, the absorption being characteristic of nitrogen defects [13, 14] has not been registered, which indicates a low (less than 10^{16} cm^{-3}) content of the nitrogen impurity in these crystals.

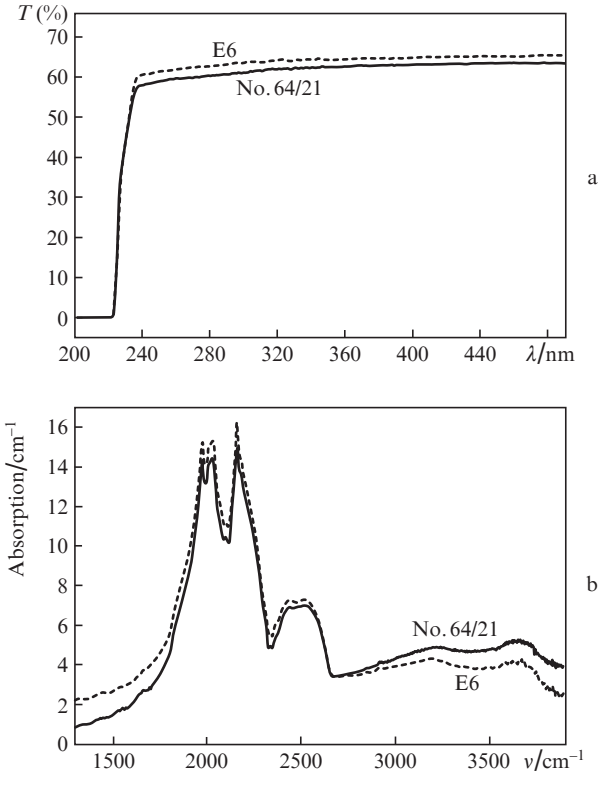

Figure 1. (a) Transmittance spectrum in the UV and visible regions, and (b) absorption spectrum in the IR region for the samples E6 and No. 64/21.

Optical scheme of the setup to implement the method of transient gratings is shown in Fig. 2. The diffraction beam splitter (*1*) splits the source light beam from a pump pulsed laser into two identical beams, which, with the use of a two-lens quartz telescope (*2*), create in the sample plane a high-quality interference pattern of the predetermined period Λ in the range of 25–75 μm, having the 100% modulation depth. Interband excitation of the sample (*3*) leads to the spatially-periodic variation in the optical properties of the material due to both the formation of the FCC plasma and the heat release caused by FCC nonradiative recombination. To study the relaxation process of the induced grating, a cw laser ($\lambda = 473$ nm) is used, the beam of which experiences diffraction on the transmission-type transient grating. The intensity of the first-order diffraction is recorded by the photodetector (*4*) in time domain.

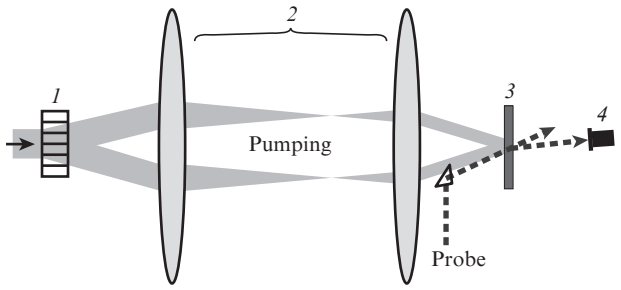

Figure 2. Experimental scheme for studying photoinduced diffraction: (*1*) diffractive beam splitter; (*2*) telescope; (*3*) sample; (*4*) photodetector.

To excite the FCCs in the samples at the wavelengths of 213 and 266 nm, a 60-ps laser pulse from the actively mode-locked Nd : YAG laser was used. The probe beam transmitted through the sample (in the study of induced absorption) or the beam of the first-order diffraction (the TG method) were detected with the use of the Hamamatsu H6780-20 photomultiplier tube (PMT). To exclude parasitic overload of the PMT, the probe laser radiation was synchronously modulated in amplitude using an acoustooptic modulator (not shown in Fig. 2). Signal accumulation and processing were conducted with the Tektronix TDA-3032B digital oscilloscope (300 MHz bandwidth). The pulse response function width for the recording system was 3.4 ns (FWHM).

For reliable detection and processing of the diffraction signal by the photo-recording apparatus in use, the TG diffraction efficiency η should be no less than 10^{-5}. This value, according to the known formula $\eta = (\pi d \Delta n/\lambda)^2$ [15], where d is thickness and Δn is the induced refractive index amplitude, is achieved at the photo-induced changes $\Delta n \approx 10^{-4}$ in the refractive index of the sample. This estimate has been made for the case of probing of the sample at a wavelength in the visible range and effective thickness of the grating defined by

the absorption coefficient α at the wavelength of 213 nm, $d = 1/\alpha_{213} \approx 10^{-3}$ cm [16].

According to the Drude–Lorenz model, the photo-induced change Δn_{fc} in the refractive index, caused by the FCC generation, is negative and defined by the relation

$$\Delta n_{fc} = n_{eh} N = \frac{-Ne^2}{2nm_{eh}\omega^2\varepsilon_0}, \quad (1)$$

where n_{eh} is the refractive index change due to the generation of one electron–hole pair; e is the electron charge; $n = 2.4$ is the refractive index of diamond at the wavelength of probe radiation; m_{eh} is the effective mass of the electron–hole pair; ω is the frequency of probe radiation; and ε_0 is the vacuum permittivity. Using the data [11, 17], we obtain for diamond $n_{eh} \approx 3\times10^{-22}$ cm^3. Therefore, to form a signal with the amplitude sufficient for registration, one has to ensure $N > 0.3\times10^{18}$ cm^{-3}. With the photon energy of 10^{-18} J (5.8 eV) at the wavelength of 213 nm, this FCC concentration is achieved at the volumetric density of the absorbed energy of pumping no less than 0.3 J cm^{-3}.

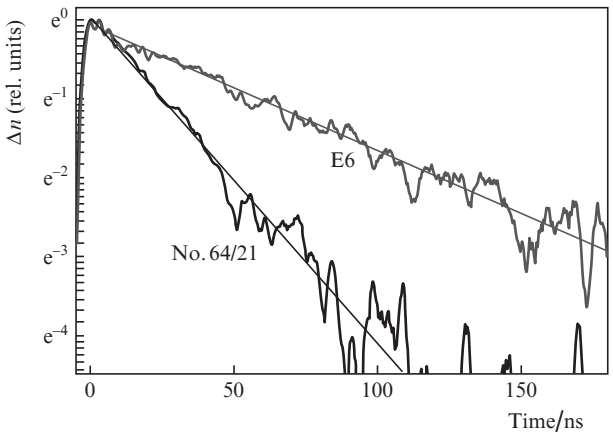

Figure 3. Kinetics of the normalised amplitude of the induced refractive index Δn for samples E6 and No. 64/21 presented in the semilogarithmic scale and approximated by the method of least squares for exponential damping. The grating period is $\Lambda = 75$ μm, the FCC initial concentration is $N \approx 7\times10^{17}$ cm^{-3}, and $E_s = 50$ mJ cm^{-2}.

3. Investigation of the diffraction kinetics

The initial transmittance T of the samples under conditions of low fluence E_s at a wavelength of 266 nm on the surface was approximately 60% (Fig. 1a). Since the absorption coefficient at 266 nm is negligible, the optical losses in the samples are due to internal scattering and Fresnel reflection from two faces of the plates for $n = 2.6$ at that wavelength [18]. It was established experimentally that the increase in the excitation energy E_s to 50 mJ cm^{-2} results in the decrease in the sample transmittance by 40%. From the known transmittance and Fresnel reflection losses (36%), it is easy to find the fraction of absorbed energy ξ and the effective absorption coefficient α, which under these conditions and at the sample thickness $h = 0.05$ cm constitute 30% and 7 cm^{-1}, respectively. In accordance with the known values of the coefficient of two-photon absorption for diamond $(1–2)\times10^{-9}$ cm W^{-1} at the wavelength of 266 nm [19, 20] and taking into account the incident radiation intensity $\sim1\times10^9$ W cm^{-2} in our experiment, the calculated absorption coefficient amounts to 1.2 cm^{-1}. The difference between the calculated and experimental values can be explained by insufficient accuracy of the energy measurement and additional contribution of the inverse bremsstrahlung absorption, leading to some heating of the plasma. In our case, the measurements of the FCC parameters were carried out on the nanosecond time scale, when the plasma can be considered already cold, since the time of its cooling due to electron–phonon interaction amounts to picoseconds.

The absorption coefficient of 7 cm^{-1} provides a sufficient for measurement and, at the same time, soft bulk excitation of the samples with approximately uniform in-depth FCC concentration. The use of this regime of excitation of the bulk phase gratings contributes to reducing the error in quantitative evaluation of dynamic parameters of the FCC plasma. At $E_s = 50$ mJ cm^{-2}, the averaged volume density of the energy absorbed in the sample is $E_v = \xi E_s/h = 0.3$ J cm^{-3}, whilst the estimated amplitude of the change in the diamond refractive index, caused by generation of the carriers, is of the order of 10^{-5}.

The kinetics of changes in the amplitude of the induced refractive index, registered during the first 50–100 ns after the excitation pulse and caused by formation and subsequent decay of the FCC grating, is presented for two samples in Fig. 3. As is shown below, the positive contribution of the thermal grating to the total change in the refractive index is insignificant. In both samples the decay law of Δn is close to exponential, with the constants τ_g equal to 56 and 24 ns for the samples E6 and No. 64/21, respectively. It was established experimentally that the TG lifetime depends linearly on the square of its period, which indicates the presence of the diffusion contribution to the relaxation of the Δn value. With the use of all the kinetics recorded at different periods Λ, two linear approximations of $\tau_g^{-1}(\Lambda^{-2})$ were plotted (Fig. 4), in accordance with the relation [11]

$$\tau_g^{-1} = \tau_r^{-1} + \tau_d^{-1}, \quad (2)$$

where τ_r is the FCC recombination time, and

$$\tau_d = \Lambda^2(4\pi^2 D)^{-1} \quad (3)$$

is the FCC diffusion time.

As follows from the slope of the graph in Fig.4, both samples have similar D values (20.3 and 18.9 cm^2 s^{-1} for the samples No. 64/21 and E6, respectively). Almost the same diffusion coefficient (19 cm^2 s^{-1}) was obtained earlier in paper [21] for polycrystalline CVD diamond at room temperature and similar experimental conditions. The linear dependences in Fig. 4 intersect the ordinate axis ($\Lambda \to \infty$) at the points $1/\tau_g = 0.033$ and 0.0053 ns^{-1}, which implies that the lifetime τ_r of the charge carriers in the samples No. 64/21 and E6 is equal to 30 и 190 ns, respectively.

The kinetics of the same processes, as in Fig. 3, is represented on the sub-microsecond linear scale in Fig. 5. The signal $\Delta n(t)$ has two components located on the opposite sides of the horizontal line of homodyne (Fig. 5a). The negative signal ($\Delta n < 0$) with a large amplitude is formed by the FCC grating during the time up to 100 ns, whilst the weakly positive ($\Delta n > 0$) signal with a maximum at the time moment $t \approx 180$ ns and the duration $\tau_{th} \approx 160$ ns has a thermal nature and is conditioned by the nonradiative recombination of the charge carriers. The bipolarity of the electronic and thermal components of the signal is due to the fact that the photoinduced electronic and thermal indices of refraction in diamond have opposite signs

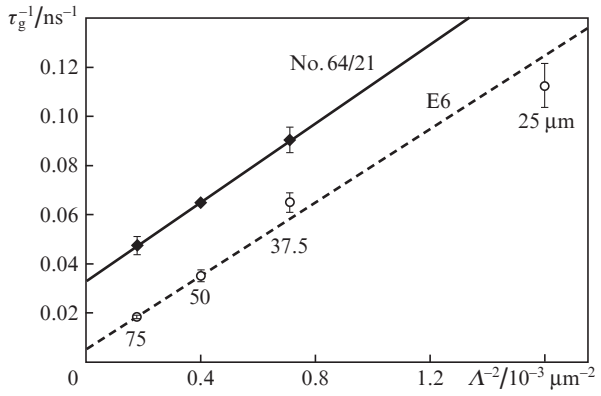

Figure 4. Dependence of the inverse lifetime τ_g^{-1} of the electronic grating on the inverse square of its period Λ^{-2} at the excitation wavelength of 266 nm for samples No. 64/21 and E6. The graph shows the grating periods in μm; $E_v = 0.45$ J cm^{-3}.

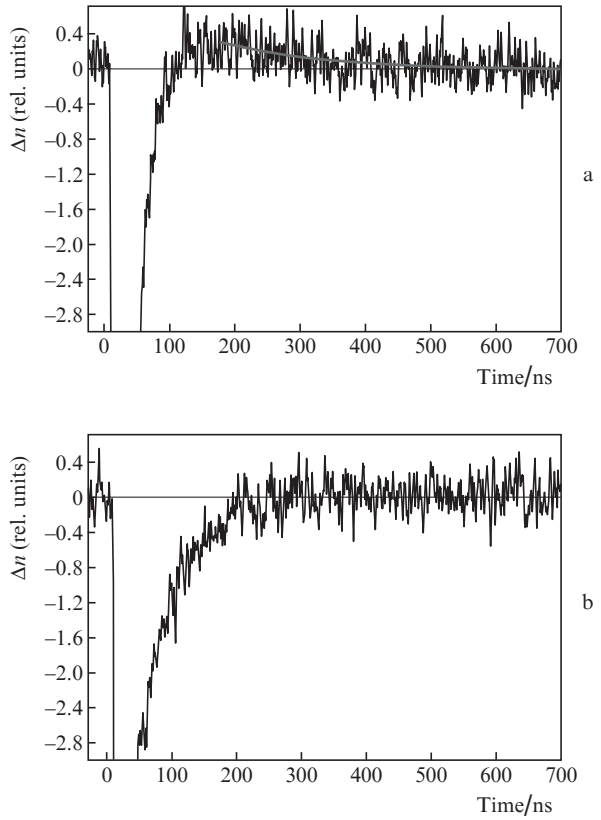

Figure 5. Kinetics of the amplitude of the induced refractive index for samples (a) No. 64/21 and (b) E6 in linear scale. On the graph for sample No. 64/21, along with a large signal down from the electronic grating, a thermal component with the lifetime of about 150 ns is visible (its damping is approximated by an exponent). The volume density of the absorbed energy $E_v = 0.45$ J cm^{-3}, the pump wavelength is 266 nm, and $\Lambda = 75$ μm.

[22]. The relative amplitude of the thermal grating is much less than that we have observed previously in polycrystalline CVD diamond, where the thermal and electron diffraction components were comparable in efficiency [22]. The thermal grating in sample E6 is inefficient and does not stand out against the background noise (Fig. 5b).

The observed amplitude peculiarities of the thermal grating in the samples we have investigated are due to the fact that its diffraction efficiency depends on the ratio of the lifetimes of electronic and thermal components. In the general case, the main sources of the heat release in the diamond volume are the nonradiative recombination of the charge carriers and the inverse bremsstrahlung absorption by the free carriers of a fraction of the pump energy with subsequent transfer of the heat to the phonon subsystem. We believe that the dominant source of the heat was recombination, since had the contribution of the inverse bremsstrahlung been significant, it would have led to a rapid formation of the effective thermal grating regardless of the FCC recombination rate, which was not observed in our experiment.

The thermal grating can be formed if the recombination time τ_r is less than the diffusion relaxation time τ_d of the FCC grating and the lifetime τ_{th} of the thermal grating. Implementation of these conditions can be enhanced by increasing the TG period. In the limiting case, when $\tau_r \ll \tau_d$ and $\tau_r \ll \tau_{th}$, all the heat released is fully spent on the formation of the thermal component of diffraction [22]. The thermal grating amplitude is small at cw pumping of the semiconductor, since it is only determined by the amount of the heat energy released during its relaxation [23].

For sample No. 64/21, which has $\tau_r = 30$ ns, $\tau_d = 70$ ns, $\tau_{th} = 150$ ns, the condition of thermal grating formation, albeit with a not large efficiency, is fulfilled. On the contrary, for a more perfect sample E6 we have $\tau_r > \tau_D$, so that the thermal grating is virtually not observed.

For the purpose of comparison with the results presented above, similar studies have been performed with excitation of the samples at the wavelength of 213 nm. In this case, the average volumetric density of the absorbed energy increased (as a result of its concentration in a thin layer with a thickness of about 3 μm) up to about 50 J cm^{-3}, and, consequently, the FCC concentration increased up to 5×10^{19} cm^{-3}. At the TG period $\Lambda = 50$ μm, the nonexponential decay kinetics $\Delta n(t)$ with local constants of relaxation increasing from the initial to final part of the kinetics were registered. Within the initial time interval from 0 to 40 ns, the curves can be satisfactorily approximated by an exponential law with the relaxation time of 10 and 15 ns for samples No. 64/21 and E6, respectively. For comparison, in the case of excitation of the samples having the same grating period at the wavelength of 266 nm, the damping time increased up to 15 and 30 ns (see Fig. 4); the relaxation time data are given in Table 1.

Table 1.

Sample	D/cm^2 s^{-1}	τ_r/ns	τ_d/ns	τ_{th}/ns
No. 64/21	20.3	30	70	~150
E6	18.9	190	65	—

Note: the pump wavelength is 266 nm, the absorbed energy density is $E_v = 0.45$ J cm^{-3}.

Note that in paper [24], under the conditions of femtosecond excitation and higher concentration of free charge carriers (~3×10^{20} cm^{-3}), the refractive index change $\Delta n = -0.04$ was achieved in a sample of monocrystalline diamond, whilst the measured recombination time was 20 ps. The difference in recombination time is too large to be explained by different concentrations of free carriers. We assume that the main factors affecting the FCC recombination time are not so much the excitation conditions and carrier concentration, but, more likely, the peculiarities of internal structure of particular samples. As is known, the FCC recombination time in diamonds

with a different structure and content of defects can vary by several orders of magnitude [25–27]. In particular, the FCC lifetime achieves the value of 1 μs for ultra-pure single-crystals of CVD diamond with the content of nitrogen impurity less than 10^{15} cm^{-3} and a low dislocation density [27].

4. Kinetics of induced absorption

When the grating period is $\Lambda \to \infty$ (spatially uniform excitation), the electronic component lifetime is only determined by the FCC recombination time, since the diffusion component is missing. In such an embodiment of the sample excitation one can put that, provided the FCC concentration is rather small, the logarithm of the relative transmittance $T_0/T(t)$ depends on time exponentially [28]:

$$\ln(T_0/T(t)) \approx \exp(-t/\tau_r). \quad (4)$$

Kinetics of the transmittance change in sample E6 for the pump energy density of 50 and 70 mJ cm^{-2} in the uniformly irradiated spot is presented in Fig. 6. The dependence of τ_r on the FCC concentration leads to the fact that the signal relaxation obeys a nonexponential law, with a gradual slowdown in the recombination rate. This is the reason why the values of τ_r were determined on the initial [from 0 to 200 ns (τ_{r1})] and the final [from 600 to 800 ns (τ_{r2})] segments of kinetics, where the noise level is still acceptable for the measurement.

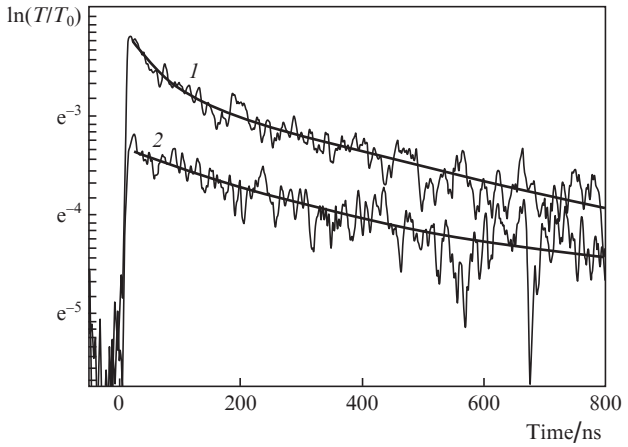

Figure 6. Kinetics of the induced transmittance for sample E6 at (*1*) E_s = 70 mJ cm^{-2}, E_v = 0.6 J cm^{-3}, τ_{r1} = 140 ns, τ_{r2} = 600 ns and (*2*) E_s = 50 mJ cm^{-2}, E_v = 0.45 J cm^{-3}, τ_{r1} = 250 ns, τ_{r2} = 1200 ns.

Some discrepancy in τ_r for two experiments with sample E6, performed at the same excitation energy (250 ns without the grating vs. 190 ns under the condition of grating excitation) is conditioned by the fact that, at the close pump-spot-averaged energy values for both cases, the local energy density at the maxima of the spatially periodic pumping in the TG method is twice higher compared to its average value. The nonlinear dependence of τ_r on the local FCC concentration deforms initially the sinusoidal shape of the grating lines and reduces the recombination time. This is consistent with our measurements of τ_{r1}, performed with increasing excitation energy density up to 70 mJ cm^{-2} (see Fig. 6). For samples E6 and No. 64/21, we have obtained τ_r = 140 and 40 ns, respectively, which is close to the values found in the experiments on diffraction with E_v = 0.45 J cm^{-3}.

5. Conclusions

By means of the methods of transient gratings and induced absorption, the kinetics of the FCC plasma generated by picosecond laser pulses in two samples of high-quality single crystals of CVD diamond at the concentration of nitrogen defects less than 10^{16} cm^{-3} has been investigated.

It is shown that, when pumped at the wavelength of 266 nm with initial (maximum) FCC concentration no more than 7×10^{17} cm^{-3}, samples No. 64/21 and E6 have similar diffusion coefficients (20.3 and 18.9 cm^2 s^{-1}), but significantly differ in the FCC recombination time (30 and 190 ns). In both crystals, the increase in the FCC concentration up to 5×10^{19} cm^{-3}, when the FCCs are excited in the fundamental absorption band with the wavelength of 213 nm, results in a reduction of the FCC grating lifetime. The characteristic times of 140–250 ns of the induced absorption existence are generally consistent with those obtained by the TG method.

Unlike previously studied diamonds containing the defects or having the polycrystalline structure, the heat release resulted from the FCC recombination in diamonds of more perfect structure and low content of defects is not adiabatic. The comparatively long recombination leads to the fact that the processes of electronic and thermal diffusion substantially reduce the efficiency of the thermal grating down to its disappearance.

Acknowledgements. This work was supported by the Russian Science Foundation (Grant No. 14-12-01403). E.V.I. and I.G.K. are grateful for the support of the Belarusian Republican Foundation for Basic Research (Grant No. F13K-063).

References

1. Othonos A. *J. Appl. Phys*., **83** (4), 1789 (1998).
2. Garnov S.V., Ritus A.I., Klimentov S.M., Pimenov S.M., Konov V.I. *Appl. Phys. Lett*., **74**, 1731 (1999).
3. Amal'skaya R.M., Gamarts E.M. RF Patent 2006987, H01L 21/66 (1994).
4. Vaitkus Yu., Petrauskas M., Jarašiunas K. *Fiz. Tekh. Poluprovodn*., **16**, 1013 (1982).
5. Bergner H., Brückner V., Supianek M. *IEEE J. Quantum Electron*., **QE-22**, 1306 (1986).
6. Schetzina J.F., McKelvey J.P. *Phys. Rev. B*, **2**, 1869 (1970).
7. Malinauskas T., Jarašiūnas K., Ivakin E.V., Tranchant N., Nesladek M. *Phys. Status Solidi A*, **207**, 2058 (2010).
8. Jarašiūnas K., Malinauskas T., Aleksejunas R., Ivakin E., Ralchenko V., Gontar A. *Mater. Sci. Forum*, **600–603**, 1301 (2009).
9. Malinauskas T., Jarašiūnas K., Ivakin E., Ralchenko V., Gontar A., Ivakhnenko S. *Diamond Relat. Mater*., **17**, 1212 (2008).
10. Jarašiūnas K., Stonys S., Širmulis E. *IEEE J. Quantum Electron.*, **QE-22**, 1341 (1986).
11. Ščajev P., Gudelis V., Ivakin E., Jarašiūnas K. *Phys. Status Solidi A*, **208**, 2067 (2011).
12. Bolshakov A.P., Ralchenko V.G., Polskiy A.V., Konov V.I., Ashkinazi E.E., Khomich A.A., Sharonov G.V., Khmelnitsky R.A., Zavedeev E.V., Khomich A.V., Sovyk D.N. *Plasma Phys. Rep*., **38**, 1113 (2012).
13. Nistor S.V., Stefan M., Ralchenko V., Khomich A., Schoemaker D.J. *Appl. Phys*., **87**, 8741 (2000).
14. Clark C.D., Davey S.T. *J. Phys. C: Solid State Phys*., **17**, 1127 (1984).

15. Miller M. *Optische Holographie – Theoretische und experimentelle Grundlagen und Anwendungen* (München: Thiemig, 1978; Leningrad: Mashinostrenie, 1979).
16. Nesladek M., Bogdan A., Defeme W., Tranchant N., Bergonzo P. *Diamond Relat. Mater*., **17**, 1235 (2008).
17. Vavilov V.S., Gippius A.A., Konorova E.A. *Elektronnye i opticheskie protsessy v almaze* (Electronic and Optical Processes in Diamond) (Moscow: Nauka, 1985).
18. Zaitsev A.M. *Optical Properties of Diamond: a Data Handbook* (Berlin, Heidelberg: Springer-Verlag, 2001).
19. Preuss S., Stuke M. *Appl. Phys. Lett*., **67**, 338 (1995).
20. Sheik-Bahae M., DeSalvo R.J., Said A.A., Hagan D.J., Soileau M.J., Van Stryland E.W. *Proc. SPIE Int. Soc. Opt. Eng.*, **2428**, 605 (1995).
21. Ščajev P., Gudelis V., Jarašiūnas K., Kisialiou I., Ivakin E., Nesladek M., Haenen K. *Phys. Status Solidi A*, **209**, 1744 (2012).
22. Ivakin E.V., Sukhadolau A.V., Ralchenko V.G., Vlasov A.V. *Proc. SPIE Int. Soc. Opt. Eng.*, **5121**, 253 (2002).
23. Rubanov A.S., Ivakin E.V., in *Kvantovaya elektronika i lazernaya spektroskopiya* (Quantum Electronics and Laser Spectroscopy) Ed. by A.M. Samson (Minsk: Nauka i tekhnika, 1974).
24. Kononenko V.V., Zavedeev E.V., Latushko M.I., Konov V.I. *Laser Phys. Lett*., **10**, 036003 (2013).
25. Pan L.S., Kania D.R., Pianetta P., Ager III W., Landstrass M.I., Han S. *J. Appl. Phys*., **73**, 2888 (1993).
26. Malinauskas T., Jarasiunas K., Ivakin E., Ralchenko V., Gontar A., Ivakhnenko S. *Diamond Relat. Mater*., **17**, 1212 (2008).
27. Isberg J., Hammersberg J., Johansson E., Wikström T., Twitchen D.J., Whitehead A.J., Coe S.E., Scarsbrook G.A. *Science*, **297**, 1670 (2002).
28. Roth T., Laenen R. *Opt. Commun.*, **189**, 289 (2001).